# Size-dependent velocity distributions and temperatures of metal clusters in a helium carrier gas

Johan van der Tol and Ewald Janssens*

*Quantum Solid-State Physics, Department of Physics and Astronomy, KU Leuven, Celestijnenlaan 200D, 3001 Leuven, Belgium*

(Received 22 February 2020; revised 15 June 2020; accepted 10 July 2020; published 10 August 2020)

Combining a laser vaporization cluster source, a velocity scan system, and a time-of-flight mass spectrometer, we measured velocity distributions of few-atom cobalt clusters ($Co_n$, $n = 6$–$60$) suspended in a helium carrier gas and expanded into vacuum. The velocity distributions provide information about the cluster size dependence of the translational temperature, flow velocity, and velocity slip with respect to the helium carrier gas. The system of clusters in a carrier gas is found to violate the equipartition theorem. Although the clusters in the expansion do not thermalize with the helium gas, they do experience significant, size-dependent internal cooling. While expanding into vacuum, the clusters collide, at least a couple of hundred times, superelastically with the carrier gas, thereby transferring internal vibrational energy into self-acceleration and increasing the flow velocity of the gas as a whole. It is also demonstrated that the proposed velocity distribution measurements can be used to test whether a source produces thermalized clusters.

DOI: 10.1103/PhysRevA.102.022806

## I. INTRODUCTION

Many gas-phase physical techniques for the production of atomic clusters exist. Irrespective of the method of choice, the production of clusters, which are particles composed of a few atoms to a few hundreds of atoms, follows a similar approach [1]. Material ejected from a bulk target forms a vapor plume, which in a first step is cooled via three-body collisions involving a noble carrier gas atom, often He, such that atoms of interest aggregate into clusters. Subsequently, expansion from the high-pressure region inside the source into vacuum creates a molecular beam of clusters [2]. The temperature of clusters produced by gas-phase physical techniques is typically not well known [3]. Inside the source, the condensation energy causes strong internal heating of small clusters with a limited heat capacity, which makes it difficult to thermalize an entire cluster distribution. The formation of larger clusters requires more condensation events. Larger clusters are likely formed later in the expansion, where there are fewer collisions with the carrier gas. In this case they are hotter than smaller clusters [4]. Moreover, the clusters cool via collisions with the carrier gas in the expansion, but the expansion conditions depend on the particle size [5]. In addition, the number of collisions decreases continuously while expanding into vacuum. In such systems, energy can no longer be effectively equilibrated between the different degrees of freedom, meaning that temperature is not a well-defined concept and loses its usual meaning. Instead, effective temperatures are sometimes employed corresponding to the different quantum states (i.e., $T_{\mathrm{rot}}$, $T_{\mathrm{vib}}$, etc.) [4].

Although the temperature of clusters in a molecular beam is difficult to control, it is a crucial for the interpretation of many experiments. This is particularly true for reactivity experiments, where the reaction rates are dependent on the initial temperature of the clusters [6–8]. Variation of cluster temperature with size can cause confusion if properties such as reactivity are compared for clusters of different sizes [9]. Knowledge about the temperature of clusters in a molecular beam is also crucial for the interpretation of electric- and magnetic-deflection experiments [10–13]. Inconsistencies between magnetic moments for cobalt clusters obtained by beam-deflection experiments in different groups likely originate from difficulties to control the internal temperature of the clusters [14]. The common practice is to assume that clusters are thermalized to the source, which has been shown to be the case for temperatures above 30 K if the dwell time in the source is sufficiently long [15,16]. After expansion the vibrational temperature is assumed to remain at the source temperature since vibrational degrees of freedom are not efficiently cooled [17], while the rotational temperature is reduced [11,12]. Size dependencies are usually ignored. Clearly, a better control over the size-dependent cluster temperature would be beneficial.

Given the difficulties in thermalizing clusters, a method to check whether these assumptions are valid would be a significant improvement over current practice. Several methods to gain information about cluster temperature have been proposed, as summarized by Makarov in two review papers [18,19]. Most techniques are experimentally challenging and not available in common cluster setups. Milani and de Heer [20] used argon tagging to obtain relative information of the temperature, but they also had to rely on simple gas dynamics to predict the absolute temperatures.

In the current work we study the collisions of clusters with helium carrier in an expansion and measure the size-dependent velocity distribution of the clusters in the molecular beam. A methodology is proposed, allowing (1) to test thermalization of the clusters in the source, (2) to determine the amount of internal energy released to the carrier gas, and (3)

*ewald.janssens@kuleuven.be

 

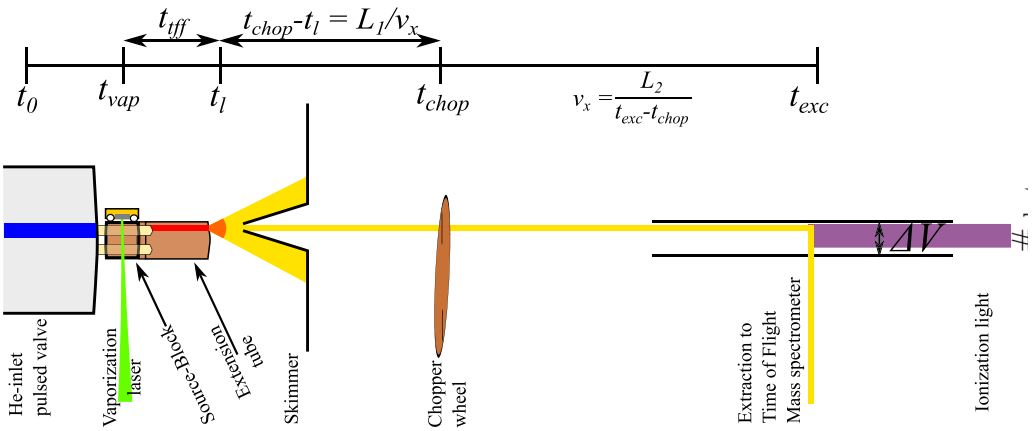


FIG. 1. Time line of the experiment. Controlling $t_{\text{chop}}$ and $t_{\text{exc}}$ effectively provides control over $t_{tff}$ and $v_x$. By measuring the cluster abundances at different times, the velocity distributions are recorded. The high-pressure regime is depicted in red, the interacting regime in orange, and the free-flight regime in yellow.

to estimate the number of collisions the clusters underwent during expansion. We demonstrate that the equipartition theorem, which assumes that energy is shared equally among all degrees of freedom, loses its validity in cluster beams if the particles are significantly bigger than a few atoms. This particularly holds for the translational temperature, which we find to barely change from its value in the source. At the same time we find that a significant amount of energy is released from the clusters in the expansion, which can only be attributed to a reduction in the internal temperatures.

## II. EXPERIMENTS

### A. Experimental setup

A broad size range of cobalt clusters is produced in a laser vaporization source. The cluster source consists of a copper source block, which contains the formation channel, and a 11-cm-long copper extension tube with a diameter of 3 mm. The open end of the extension tube serves as a nozzle. Atoms are evaporated from a bulk target by focusing the second harmonic of a pulsed Nd-YAG laser. A short pulse of helium gas carries the evaporated atoms into the extension tube. During this process, the evaporated metal atoms collide with the helium atoms, loose kinetic energy, and cluster together via three-body Co-Co-He collisions. After the growth process, the clusters are cooled by the more frequent two-body collisions with He gas, which in itself thermalizes with the walls of the source block. After formation, the clusters are released into the vacuum.

The temperature of the source is controlled by the combination of a cold finger (Coolpower 10 MD, Leybold GmbH) and resistive heating. The cold finger is connected to the source via a copper braid that spans the entire length of the extension tube. Two temperature sensors monitor the temperature of the source; one is mounted on top of the source block ($T_{S,\text{Block}}$) and the other at the end of the extension tube ($T_{S,\text{Ext}}$).

The cluster beam experiences an expansion, cooling down the translational temperature. The centerline of the gas expansion is selected by a skimmer. At this point the clusters have reached free flight at constant velocity. A chopper wheel with a small hole, rotating at 200 Hz, is located 35 cm after the skimmer. The chopper restricts the cluster beam passage to a fixed time. When the neutral clusters reach the extraction zone, located 1.34 m downstream, they are ionized by an excimer laser (6.42 eV photons), and their mass distribution is probed by time-of-flight mass spectrometry. The excimer laser is expanded (fluence $<2.3$ mJ cm$^{-2}$) to avoid multiple photon absorption and fragmentation of post-ionized clusters. The energy of a single photon is for the studied cobalt clusters below the sum of the ionization and the dissociation energy [21,22].

### B. Velocity scan method and velocity distributions

The time line of the experiment, illustrated in Fig. 1, can be split up into three regimes: (i) the high-pressure regime, where the clusters are inside the extension tube of the source (in red); (ii) the interacting regime, where the clusters have entered the vacuum chamber but are still colliding with the helium gas (in orange); and (iii) the free-flight regime, where the clusters travel at a constant velocity and the velocity distribution is frozen (in yellow). The last two regimes form the expansion. The time between the vaporization due to the laser firing and the start of the free-flight regime is defined as the time to free flight $t_{tff}$. We estimate that this regime starts about one centimeter behind the nozzle [23]. In other studies one uses the residence time in the source instead of $t_{tff}$ [24]; however, this ignores the time spent in the interacting regime, where a constant velocity is not yet achieved. Because the chopper wheel is located about 35 cm behind this point (36 cm behind the nozzle), the relative error on its position is small. An estimate for $t_{tff}$ can be made, assuming a constant velocity from the start of the free-flight regime to the chopper wheel.

Although the experiment produces clusters having a range of $t_{tff}$ values, a combination of control over the moments in time that the chopper wheel opens, $t_{\text{chop}}$, and that the ionization laser fires, $t_{\text{exc}}$, allows selecting only clusters with a well defined $t_{tff}$. The combination of $t_{\text{chop}}$ and $t_{\text{exc}}$ defines the velocity $v_x$:

$$v_x = \frac{L_2}{t_{\text{exc}} - t_{\text{chop}}}, \tag{1}$$

where $L_2 = 1.344$ m is the distance between the chopper wheel and extraction zone. Therefore we can select clusters with a fixed $v_x$ and count their abundance.

By recording the abundance of clusters of a certain size and $v_x$ at a fixed $t_{tff}$, one obtains the cluster-size-dependent velocity distribution. To control $t_{tff}$, the distance $L_1 = 0.346$ m between the chopper wheel and the source nozzle is used. Although it is not exactly known where between the nozzle and the chopper the free flight starts, the distance between the nozzle and skimmer is short enough to create a smaller uncertainty than the one created by the nonzero duration of the chopper-wheel opening. The location where the particles start their free flight is called the quitting surface $q$. The moment in time that the particles start their free flight is called $t_q$ in reference to $t_0$:

$$t_q = t_{\text{chop}} - \frac{L_1}{v_x}. \tag{2}$$

This allows determining $t_{tff}$:

$$t_{tff} = t_q - t_{\text{vap}}, \tag{3}$$

where $t_{\text{vap}}$ is the moment the vaporization laser fires. This ends up with the following relation:

$$t_{tff} = \left(1 + \frac{L_1}{L_2}\right) t_{\text{chop}} - \frac{L_1}{L_2} t_{\text{exc}} - t_{\text{vap}}. \tag{4}$$

Formulas (1) and (4) allow us to calculate $v_x$ and $t_{tff}$ for any combination of $t_{\text{vap}}$, $t_{\text{exc}}$ and $t_{\text{chop}}$.

A selection of the measured $x$-velocity distributions of $Co_n$ clusters are provided in Fig. 2. They are measured by scanning $v_x$, while keeping $t_{tff} = 556$ $\mu$s constant. The experiment was performed for measured source temperatures of $T_{S,\text{Block}} = 79$ K and $T_{S,\text{Ext}} = 71$ K. The wall of the formation channel at the inside of the source may be slightly warmer due to the introduction of room-temperature carrier gas and due to the power of the vaporization lasers.

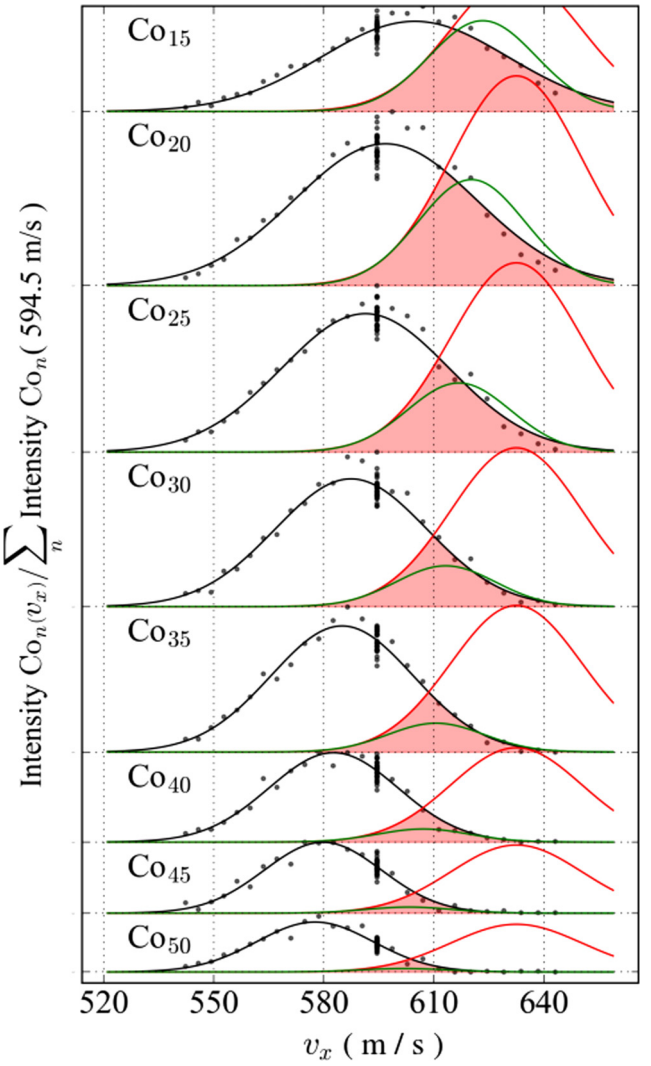


FIG. 2. Measured $x$-velocity distributions for $Co_n$ clusters with $n = 15, 20, 25, 30, 35, 40, 45, 50$. The red line represents a helium distribution at $S = 25$. The overlap is shaded in red and gradually becomes less as the mass increases. For every $v_x$ a reference mass spectrum at 595 m/s was measured to monitor cluster production, hence also the large number of data points around that value. The $y$ axis represents the intensity of a cluster mass in the mass spectrum, divided by the sum over all masses in the corresponding reference at 595 m/s. The green lines are the product of the helium distribution and the fitted velocity distributions.

## III. A GAS IN MOTION

### A. Thermodynamics of molecular beams

The thermodynamics of molecular-beam expansions of atoms and small molecules is known from gas dynamics investigations in the seventies and eighties [25–29]. Molecular beams were created by expanding particles from a source into a vacuum chamber. The experimental observations could well be described by the sudden freeze model. This model assumes a high collision regime when the particles leave the source, but due to expansion "suddenly" there are no collisions anymore, and the particles in the molecular beam find themselves in free flight. This is different from traditional continuous flow equations, which require sufficient collisions. An extended description can be found in a book by Hans Pauly [30].

Accelerating heavy particles in a beam dominated by a light carrier gas was described already in 1955 by Becker [31,32]. Becker used a very dilute solution of heavy particles suspended in a light carrier gas. The heavy particles were accelerated by collisions with the light carrier gas and finally approached the flow velocity of the light carrier gas. However, the coupling between the two turned out to be incomplete and a small mismatch in velocity between the light and heavy gas was observed [33]. This mismatch became known as the velocity slip. In He-Ne mixtures, with the mass of neon being an order of magnitude larger than that of helium, the velocity slip was never larger than 20% [34]. These understandings became textbook material [30] and the results were, without solid motivation, extrapolated to clusters in a molecular beam.

The behavior of clusters in a carrier gas is, however, distinct from that of molecular-beam expansions of gas mixtures of atoms or small molecules due to the large number of vibrational degrees in a cluster. If the velocity slip between the heavy clusters and the carrier gas is large, the clusters do not thermalize with the helium during the expansion. Obtaining

information about cluster temperature in a molecular beam is more complicated than for atoms or small molecules for two reasons: First, clusters possess four temperatures, two translational, one in the direction of the beam and one perpendicular to it, and two internal temperatures, the rotational and vibrational temperatures. The second complication is that it is hard to quantify the vibrational and rotational cooling in the expansion. Experiments regarding delayed ionization rates suggested the internal vibrational temperature not to cool for clusters [17].

### B. Velocity distribution of a gas in an expansion

The velocity of a one-dimensional gas can be described by the Maxwellian distribution [35]

$$f(v_x)dv_x \propto \exp\left(-\frac{m{v_x}^2}{2kT_x}\right)dv_x = \exp\left(-\frac{{v_x}^2}{{v_{w,x}}^2}\right)dv_x, \quad (5)$$

where

$$v_{w,x} = \sqrt{\frac{2kT_x}{m}} \quad (6)$$

is introduced as the width of the distribution, with $T_x$ being the translational temperature. If there are enough collisions between the particles, the equipartition theorem can be applied, $T = T_x = T_y = T_z$, and one obtains the commonly known Maxwell-Boltzmann speed distribution. However, this description is invalid in a molecular-beam expansion in the $x$ direction, where the gas rapidly becomes dilute and the resulting collision rate is so low that $T_x \neq T_y = T_z$. Therefore, one has to treat every direction separately using Eq. (5). The average velocity in Eq. (5) is $\overline{v_x} = 0$, which is only true if the observer is in the same frame of reference as the gas. If the gas flows from one location to another, like in this experiment, the observer is usually not in the same frame of reference, and the gas can be accelerating as a whole. The acceleration takes place irrespective of the spread in velocity for a distribution of identical particles, which is associated with its temperature. Therefore it makes sense to introduce a flow velocity $\vec{w} \equiv \overline{v}$. Here, the $x$ axis is taken as the central axis in the experiment, meaning $\vec{w} = (w, 0, 0)$. For a flowing gas, Eq. (5) can be rewritten as

$$f(v_x)dv_x \propto \exp\left(-\frac{(v_x - w)^2}{{v_{w,x}}^2}\right)dv_x. \quad (7)$$

The speed ratio, defined as $S = w/v_w$, is related to the Mach number $M$ by $S = \sqrt{\gamma/2}M$, with being $\gamma$ the specific-heat ratio. For heavy particles such as clusters, $\gamma \approx 1$ and $S\sqrt{1/2}M$ [30]. Since $v_w$ is a measure of the chaotic temperature-related velocity and the flow velocity $w$ is a measure of the non-chaotic non-temperature-related systematic flow, the speed ratio is a measure of how nonchaotic the motion of the gas is. A normal chaotic gas in a chamber at rest has $S = 0$, while a strongly directional gas has $S \gg 1$.

### C. Sudden freeze model

To clarify what happens in a gas expansion, two extremes are considered: continuous flow and collision free expansion. In the latter case, each particle is in free flight and moves along a straight line. In a vacuum environment this is elementary decompression, which is well known to result in a decrease of the temperature without decreasing the total energy of the system. Decompression leads in its essence to a smaller number of particles per unit volume, thus decreasing the spread of the kinetic energy. As temperature is a local property, the lower temperature is the result of the more narrow velocity distribution, as the range of velocities that allow particles to reach each local point in space becomes narrower the further the particles move.

In the case of the expanding beam traveling in the $x$ direction, the cooling can be understood by tracking the paths of particles and considering $v_{w,z}$, the width of the velocity distribution perpendicular to the beam. After traveling a distance $x$, the range of velocities that can make it to a certain $z$ position reduces, causing a narrower $v_z$ velocity distribution. If the particles move in straight lines and originate from a nozzle opening with size $d$, the velocity perpendicular to the beam is constrained: $w_z - w_x d/2x < v_z < w_z + w_x d/2x$, or $v_{w,z} < w_x d/x$. Here, $w_x$ is the flow velocity in the direction of the beam, and $w_z(z)$ is the perpendicular flow velocity required to reach a $z$ position. The measurements are performed on the axis of the beam, i.e., $z = 0$, where $w_z = 0$, and $w_x = w$. This implies $v_{w,z}$ and therefore $T_z$ decreases with distance $x$.

The main difference between the molecular beam in the collision-free expansion and an expanding ideal gas is that the decompression happens only in the $z$ and $y$ directions. In the collision-free scenario, $T_x$, the translational temperature in the direction of the beam, remains constant because there is no decompression in that direction.

The situation is very different in an interacting regime, where a gas can be described by continuous flow equations. As long as the pressure is high enough there is only one temperature $T_x = T_z = T$ and the rapidly decreasing $T_z$ is thermalizing with $T_x$ through collisions. The description of such an expansion into a vacuum is more complicated [27,30], as kinetic energy from the $x$ direction is transferred to the $z$ direction. However, the gas will become more and more dilute, meaning that the collision rate decreases rapidly with distance from the source. At some point, the number of collisions is so low that the continuous flow breaks down. Eventually, the particles will enter the collision-free regime. The velocity profile in the parallel direction is now frozen at a fixed temperature $T_x$, while the perpendicular temperature $T_z$ continues to cool along the beam axis. Splitting up the expansion in two regimes, continuous flow and free flight, with an abrupt transition between both at the quitting surface, is known as the sudden freeze model [25–27,30]. In this model $T_z = T_x$ up to the quitting surface, and after the quitting surface $T_x$ is constant (or "suddenly frozen"), while $T_z$ continues to decrease. For gases with few vibrational degrees of freedom, the sudden freeze model was used to predict velocity distributions based on known temperatures [25–27,30]. We follow the inverse approach and use the velocity distribution to obtain information about the temperature.

Considering the supersonic expansion, the anisotropic Maxwellian velocity distribution is used:

$$f(v_x, v_z) \propto \exp\left(-\frac{m(v_x - w)^2}{2k_B T_x} - \frac{m{v_z}^2}{2k_B T_z}\right). \quad (8)$$

Since only $v_x$ is scanned in the experiment, the $z$ direction can be integrated out, resulting in Eq. (7), where $T_x$ is constant after the quitting surface. Because of the frozen value, measuring $T_x$ at any point after the quitting surface allows determination of the temperature at the quitting surface, $T_q$.

## IV. CLUSTERS IN A CARRIER GAS

### A. Experimental cluster-velocity distributions

The experiment does not deal with a single gas but with a mixture of a majority of helium and a minority of clusters. The gas dynamics of atoms or molecules inside a carrier gas was so far only studied for particles that are maximally a few times heavier than the carrier gas atoms [30,34]. In that case, the flow velocity of the heavy particles is approximately equal to that of the carrier gas, aside from a limited velocity slip [30,34]. The velocity slip is larger if the mass ratio of the heavy particles to the carrier gas atoms increases. This can also be seen in Fig. 2. In this figure the red line represents a prediction for the $v_x$ distribution of the helium. It can be seen that the $v_x$ distribution of the clusters slips more as the mass of the clusters increases.

The origin of the velocity slip can be understood by considering the acceleration process during expansion. Due to its light mass, helium reaches much higher velocities than the heavy species would reach without the helium gas. Therefore, collisions are not random, but favor acceleration of the heavy species in the direction of the expansion. Only if cluster and He would reach the same velocity, the collisions become chaotic, both accelerating and decelerating, which is a requirement to change the width of the velocity distribution. Thermalization of the two gases requires the two velocity distributions to overlap. Since the collision rate is rapidly decreasing during the expansion, the velocity distribution of the heavy species cannot fully acquire the flow velocity of the carrying helium gas, which is the origin of velocity slip [30].

In Sec. IV E it will be shown that the velocity slip of mid-sized clusters (here defined as $m \gtrsim 1000$ u) is so significant that their velocity distribution has essentially no overlap with that of the helium: hereafter referred to as a fully slipped beam. In a fully slipped beam no translational cooling of the clusters occurs because of the lack of chaotic collisions. Their translational temperature remains at the value the clusters had upon leaving the source. Fitting of Eq. (7) to the measured velocity distribution yields for each cluster size the width $v_{w,x}$ and the flow velocity $w_{\mathrm{clus}}$ (see fits in Fig. 2). The mass dependence of the fitted values is presented in Fig. 3. The general trends are in line with the above qualitative arguments, i.e., for large sizes $v_{w,x}$ decreases as $1/\sqrt{m}$, while it becomes constant at small cluster sizes. According to Eq. (6), the measured $v_{w,x}$ values in Fig. 3(a) can be used to calculate the translational temperature at the quitting surface, $T_{q,\mathrm{clus}}$. The cluster-size dependence of $T_{q,\mathrm{clus}}$ is presented in Fig. 4. The flow velocities $w_{\mathrm{clus}}$ in Fig. 3(b) decrease with size, corresponding to an increasing velocity slip.

Blackbody radiation from vacuum chambers at room temperature can in principle heat up the cold clusters [36], but that effect can be ignored here since the vibrational photon absorption and emission rate of a cold cluster is expected to be around $10^{-2}$–$10^{-1}$ s$^{-1}$ [37]. This rate is too low to be significant on the timescale of the experiment (about 1 ms).

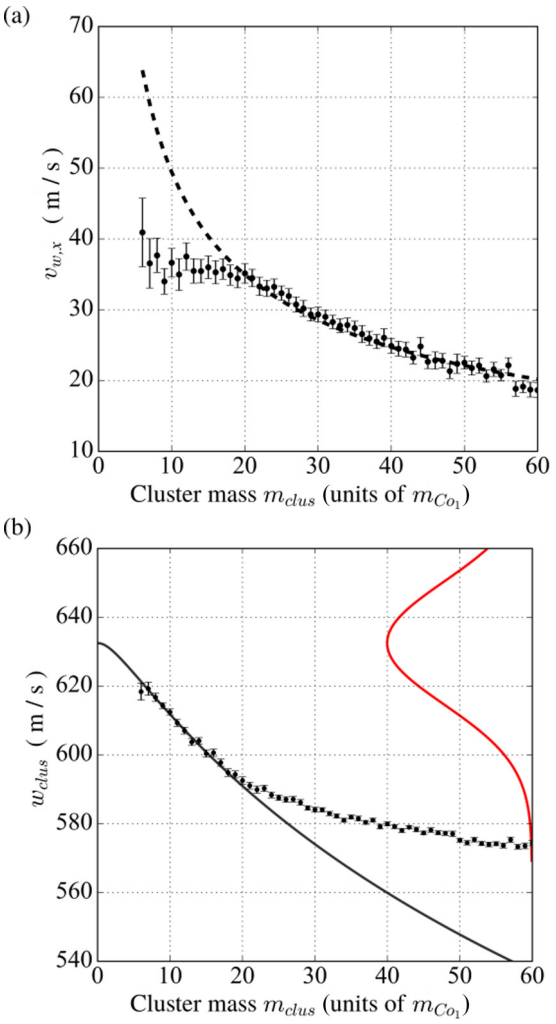


FIG. 3. (a) Width of the velocity distribution, $v_w$, and (b) flow velocity, $w_{\mathrm{clus}}$, of $\mathrm{Co}_n$ clusters as a function of their mass for $t_{tff} = 556$ $\mu$s. The dashed line in panel (a) is a fit with a $1/\sqrt{m}$ model to the $n > 20$ data, from which the source temperature is found to be $T_{S,\mathrm{clus}} = (85.9 \pm 1.1)$ K. In panel (b) the velocity distribution of the helium gas (red line on the right) for a speed ratio of $S = 25$ is added as comparison. The solid line is the elastic model (12) fit to the first 10 data points.

A more quantitative interpretation of the data is provided in the following sections. A mathematical description of the velocity slip is worked out in Sec. IV B. Section IV C relates the measured velocity slip to changes of the internal (vibrational and rotational) energy of the clusters. Section IV D discusses the number of cluster-helium collisions. Finally, Sec. IV E describes that, for heavy clusters, the translational temperature at the quitting surface is the same as that obtained in the source, which is a fingerprint to identify a well-thermalized source.

### B. Flow velocity

To quantify the flow velocity of clusters and the slip compared with the helium flow velocity, one has to consider

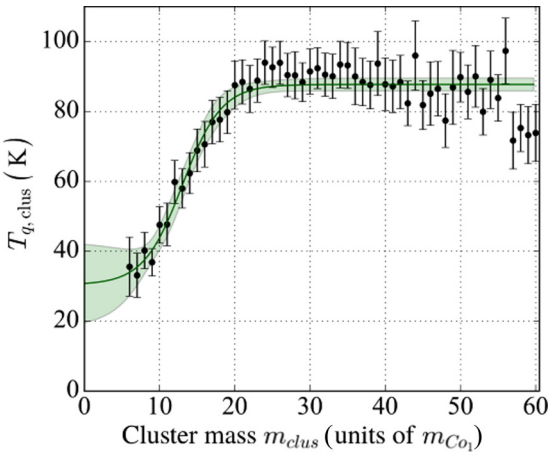


FIG. 4. Translational temperature $T_{q,\mathrm{clus}}$. It demonstrates how larger clusters do not change their translational temperature in the expansion but remain constant at the source temperature. Smaller clusters do experience translational cooling. The solid line is a working function as a guide to the eye [38].

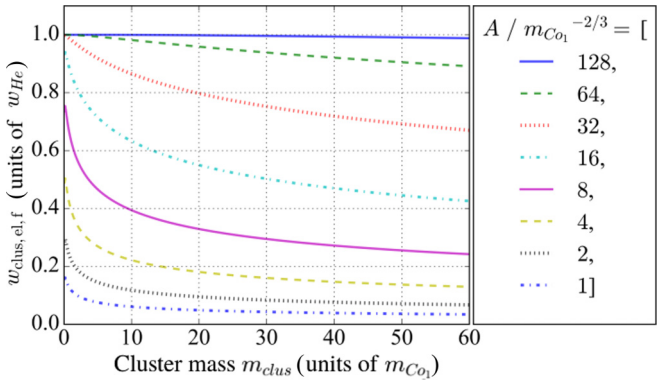


FIG. 5. Relative flow velocities of the clusters, $w_{\mathrm{clus,el}}/w_{\mathrm{He}}$, as a function of the mass of the cluster, $m_{\mathrm{clus}}/m_{\mathrm{Co_1}}$, assuming an elastic model for different values of the collision-related parameter $A$ [Eq. (11)]. $A$ is given in units of $m_{\mathrm{Co_1}}{}^{-2/3}$. If $A$ goes up, the number of collisions goes up, and the cluster flow velocity approaches the helium flow velocity. For larger masses a larger number of collisions is required for the velocity slip to vanish.

the momentum transfer from helium to the clusters. Due to the difference in flow velocity, there are more accelerating than decelerating collisions, thus there is a net number of $N$ collisions accelerating the clusters. The cluster flow velocity after $N$ collisions is given by

$$w_{\mathrm{clus}}(N) = w_{\mathrm{He}}\left[1 - \exp\left(-N\frac{m_{\mathrm{He}}}{m_{\mathrm{He}} + m_{\mathrm{clus}}}(C_R + 1)\right)\right]. \quad (9)$$

See Appendix A for a derivation of Eq. (9). It assumes a rapid acceleration of the helium to its final flow velocity. Since the cluster-cluster collision rate during the expansion is negligible, all acceleration of the clusters is caused by collisions with the helium, thus $w_{\mathrm{clus}}(N = 0) = 0$ is assumed. $C_R$ represents the coefficient of restitution and is defined as

$$C_R \equiv \left|\frac{v_{\mathrm{clus,after}} - v_{\mathrm{He,after}}}{v_{\mathrm{He,before}} - v_{\mathrm{clus,before}}}\right|. \quad (10)$$

The subscripts "before" and "after" indicate if it concerns velocities before or after the collision, respectively. If $C_R > 1$, energy is being released in the collision, known as superelastic collisions. If $C_R < 1$, energy is being absorbed, known as inelastic collisions. $C_R = 1$ is an elastic collision.

Random collisions are just as often accelerating as decelerating, affecting the width of the distribution only. Independent of the He gas density $n_{\mathrm{He}}(x)$, the net number of accelerating collisions at the quitting surface scales with the cross section of the cluster and is given by $N = N_{q,\mathrm{net}} \propto \sigma \propto {m_{\mathrm{clus}}}^{2/3}$, or $N_{q,\mathrm{net}} = A{m_{\mathrm{clus}}}^{2/3}$. This formula is the result of a finite number of helium atoms moving through a cluster cloud. $A$ is a proportionality constant that depends on the pressure, the diameter of the extension channel and its nozzle, and the detailed geometry of the cluster. Combined with Eq. (10), this yields the final cluster flow velocity after the quitting surface:

$$w_{\mathrm{clus,f}} = w_{\mathrm{He}}\left[1 - \exp\left(-A\frac{{m_{\mathrm{clus}}}^{2/3}m_{\mathrm{He}}}{m_{\mathrm{He}} + m_{\mathrm{clus}}}(C_R + 1)\right)\right]$$
$$\approx w_{\mathrm{He}}[1 - \exp(-A{m_{\mathrm{clus}}}^{-1/3}m_{\mathrm{He}}(C_R + 1))]. \quad (11)$$

Assuming elastic collisions, Eq. (11) simplifies to

$$w_{\mathrm{clus,el,f}} \approx w_{\mathrm{He}}[1 - \exp(-2A{m_{\mathrm{clus}}}^{-1/3}m_{\mathrm{He}})]. \quad (12)$$

A similar relation was found in Ref. [39]. The dependence of $w_{\mathrm{clus,el,f}}$ on $m_{\mathrm{clus}}$, as given by Eq. (12), is plotted in Fig. 5 for different values of $A$. The chosen value for $A$ was doubled until the function is similar to that of $A \to \infty$, to illustrate the behavior of the function for different values of $A$. The smaller $A$ and the higher the mass of the clusters, the larger the velocity slip.

The curves in Fig. 5 can be compared with the measured flow velocity $w_{\mathrm{clus}}$ of the $\mathrm{Co}_n$ clusters in Fig. 3. While the flow velocities of the smallest size follow the elastic model [solid line is a fit by Eq. (12)], the larger clusters are moving faster than expected based on the elastic model. This at first sight surprising result can only be explained if the collisions are not elastic but superelastic, $C_R > 1$. The higher kinetic energy after the collision comes from the internal temperature ($T_{\mathrm{vib}}$ and $T_{\mathrm{rot}}$) of the cluster, which implies that the internal temperature of the colliding cluster decreases. Only when the clusters' internal temperature reaches the low temperature of the expanded helium carrier gas do the collisions become elastic. This is discussed in more detail in Sec. IV C.

Since $N_{q,\mathrm{net}}$ scales with ${m_{\mathrm{clus}}}^{2/3}$ and the heat capacity with $m_{\mathrm{clus}}$, the heat capacity increases proportionally more with the number of atoms in the cluster. Thus larger clusters cool slower and Eq. (12) cannot be applied. Due to this slower cooling, larger clusters have a larger average $C_R$. For small clusters, superelastic energy release is less important ($C_R$ is close to one) and the scaling constant $A$ can be obtained by fitting Eq. (12) to small clusters. However, for larger clusters one needs to use Eq. (11) and assume a mass-dependent coefficient of restitution, $C_R(m_{\mathrm{clus}})$. This is consistent with work in literature regarding delayed ionization rates, where it was found that little vibrational cooling occurs in metal clusters [17].

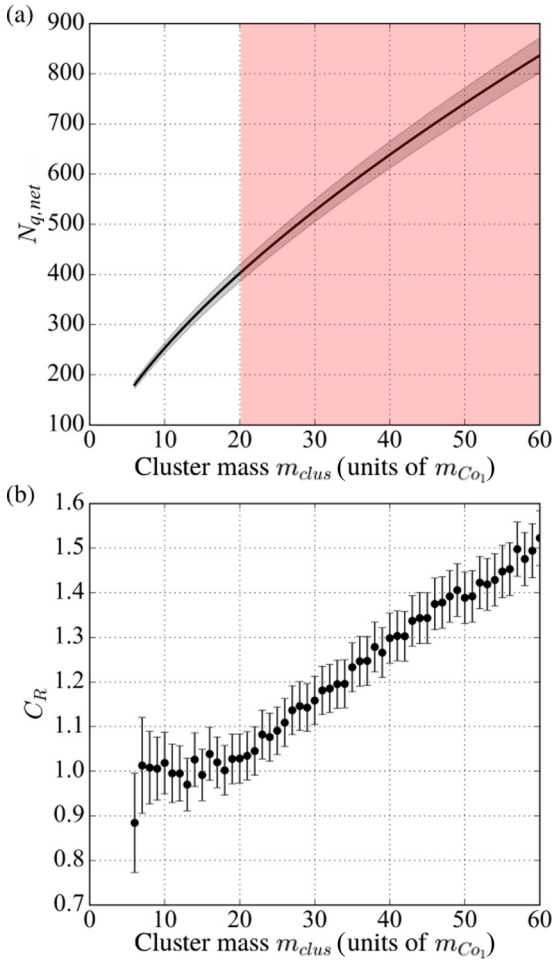


FIG. 6. (a) The minimal number of collisions, $N_{q,\mathrm{net}}$, during the expansion as a function of the cluster size. This information is retrieved from the fit with the elastic model (12) on the data in Fig. 3. The area where this corresponds to the total number of collisions is shaded. (b) Coefficient of restitution $C_R$ obtained from the data in Fig. 3 by using Eq. (13).

### C. Coefficient of restitution and energy release

Figure 3(b) allows the coefficient of restitution to be determined. Extrapolating the elastic curve for $w_{\mathrm{clus,el,f}}$ fit to the flow velocities measured for the smallest clusters and comparing it with the measured values for the clusters' flow velocity, $w_{\mathrm{clus,f}}$, it is possible to determine $C_R$ from

$$C_R = 2\frac{\ln\left(1-\frac{w_{\mathrm{clus,f}}}{w_{\mathrm{He}}}\right)}{\ln\left(1-\frac{w_{\mathrm{clus,el,f}}}{w_{\mathrm{He}}}\right)} - 1. \tag{13}$$

Equation (13) was derived by combining Eqs. (9) and (12), assuming the net number of collisions in the elastic curve $N_{q,\mathrm{net}}(m_{\mathrm{clus}}) = A{m_{\mathrm{clus}}}^{2/3}$ to be a good approximation, and taking $w_{\mathrm{He}}$ and $w_{\mathrm{clus,el,f}}$ from the elastic curve fit to the smallest clusters. From this fit with the elastic model it is possible to determine the net number of accelerating collisions, as displayed in Fig. 6(a). This figure is discussed in more detail in Sec. IV D. From the difference between the elastic model and the experimental data, it is possible to determine the

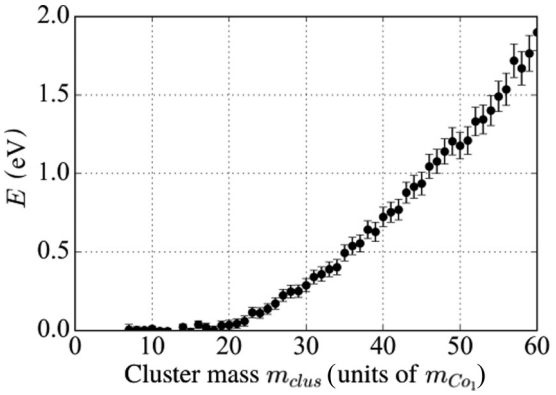


FIG. 7. $E_{\mathrm{Released}}$ determined for the same dataset as in Fig. 3. Larger clusters release more energy, which is logical given their larger heat capacity.

average coefficient of restitution $C_R$, via Eq. (13), as plotted in Fig. 6(b).

The coefficient of restitution is related to a difference in kinetic energy before and after collision. The kinetic-energy difference is given by

$$\begin{aligned}\Delta E_k &= E_{k,\mathrm{after}} - E_{k,\mathrm{before}} \\ &= \frac{\overline{m}}{2}(v_{\mathrm{clus,before}} - v_{\mathrm{He,before}})^2\left({C_R}^2 - 1\right) \\ &\approx \frac{\overline{m}}{2}[w_{\mathrm{clus}}(N) - w_{\mathrm{He}}]^2\left({C_R}^2 - 1\right),\end{aligned} \tag{14}$$

with $\overline{m} \equiv \frac{m_{\mathrm{clus}} m_{\mathrm{He}}}{m_{\mathrm{clus}}+m_{\mathrm{He}}}$ and $\Delta E_k$ is indeed zero if $C_R = 1$ [40]. Since $w_{\mathrm{clus}}(N)$ is a function of net number of collision experienced so far $N$, the energy transfer changes during the acceleration process. Opposed to the helium atoms, the clusters have internal temperatures, $T_{\mathrm{vib}}$ and $T_{\mathrm{rot}}$. If $C_R > 1$ ($C_R < 1$), the internal temperature decreases (increases) during the collisions.

The energy lost in the collisions from the internal energy results in translational energy gain. Due to conservation of momentum, this results in self-acceleration of the cluster via the collision with helium. The final flow velocity of the clusters will thus be higher after a superelastic collision than after an elastic collision, which implies a smaller velocity slip. Summing over all collisions and accounting for the change in flow velocity in every collision, the total energy released by the cluster can be determined (see Appendix B for derivation):

$$\begin{aligned}E_{\mathrm{released}} &= m_{\mathrm{clus}}(C_R - 1) \\ &\times \left\{ w_{\mathrm{clus,f}} w_{\mathrm{He}} + \frac{{w_{\mathrm{He}}}^2}{4}\left[1 - \left(\frac{w_{\mathrm{clus,f}}}{w_{\mathrm{He}}} + 1\right)^2\right]\right\}.\end{aligned} \tag{15}$$

Part of $E_{\mathrm{released}}$ will result in self-acceleration of the cluster, thus reducing the flow velocity difference and the momentum transfer compared with the fully elastic case. From the coefficient of restitution and the flow velocities it is possible to determine the amount of internal energy released by the cluster during the expansion. This is presented in Fig. 7 for the measured cobalt clusters. The figure shows that the clus-

ters are internally cooling in the expansion. We note that the actual energy being released may be smaller because it cannot be excluded that, during growth in the source, the particles already accelerate.

### D. Number of collisions

To gain further insight in the origin of the released energy, we discuss the number of collisions a cluster undergoes in the expanding gas and the role of velocity slip in this respect. The two-body collision rate of atoms in a monatomic gas at rest (or if all particles have the same flow velocity, like the helium gas), is given by [30]

$$Z = \sqrt{2} n_{\mathrm{He}} \sigma \bar{v}, \tag{16}$$

and the number of collisions $dN_{\mathrm{rest}}$ experienced by a helium atom traversing a path $dx$ by

$$dN_{\mathrm{rest}} = \sqrt{2} n_{\mathrm{He}}(x) \sigma \frac{\bar{v}(x)}{w(x)} dx. \tag{17}$$

The gas density $n_{\mathrm{He}}$ may depend on the position $x$, $\sigma$ is the geometric cross section of the particle, and $\bar{v} \equiv \sqrt{\frac{8kT}{\pi m}}$ is its mean velocity.

This description does not hold for the more complex case of a cluster ($m_{\mathrm{clus}} \gg m_{\mathrm{He}}$) moving in a gas of helium. In the case that clusters and helium form a gas at rest (or have the same flow velocity), the collision rate of a cluster with the helium, $Z_{\mathrm{clus}}$, is given by (see derivation in Appendix C):

$$Z_{\mathrm{clus}} = \frac{2\sqrt{2k_B}}{\sqrt{\pi}} \sqrt[4]{\frac{T_{\mathrm{clus}} T_{\mathrm{He}}}{m_{\mathrm{clus}} m_{\mathrm{He}}}} n_{\mathrm{He}} \sigma_{\mathrm{clus}}. \tag{18}$$

Here the subscripts "clus" and "He" refer to a single cluster and the carrier-gas atom, respectively, the temperature is the translational temperature, and $n_{\mathrm{He}}$ is the particle density for the helium gas. $Z_{\mathrm{clus}}$ scales with ${m_{\mathrm{clus}}}^{5/12}$ if one accounts for $\sigma_{\mathrm{clus}} \propto n^{2/3}$, which is valid for (nearly) spherical particles. The number of collisions the cluster undergoes traversing a path $dx$ is given by

$$dN_{\mathrm{rest}} = Z_{\mathrm{clus}} \frac{dx}{w_{\mathrm{clus}}(x)}. \tag{19}$$

Equations (18) and (19) only hold if the gasses are at rest in a frame of reference; that is, if the clusters and helium have equal flow velocity so the average net $N$ is zero and only the width of the distribution is affected. This might be the case in the high-pressure regime in the extension tube of the source, but not during expansion, where there is velocity slip, hence a significant difference in flow velocity. The different cluster and helium velocity distributions cause a great reduction of the number of collisions the cluster undergoes with respect to Eq. (19). Furthermore the aforementioned net number of accelerating collisions $N_{q,\mathrm{net}} = Am^{2/3}$ needs to be added to obtain the total number of collisions of the cluster. In the case of fully slipped clusters ($m \gtrsim 1000$ u), Eq. (19) is reduced to zero, because there is no overlap with the helium velocity distribution, and the total number of collisions becomes equal to $N_{q,\mathrm{net}}$. This corresponds to the red shaded area in Fig. 6(a). It shows that, during the expansion, clusters typically experience a couple of hundred collisions with the helium gas. By using mathematical methods it is possible to determine the number of collisions needed to thermalize the internal vibrational degrees of freedom of a cluster with its surrounding gas, as was done for example by Westergren *et al.* [5]. They found typical numbers on the order of 3000 collisions, which are not achieved for the fully slipped clusters during the collision-rich regime in the expansion. For the smaller clusters, thermalization may be better (cf. Figs. 2 and 4) because of the additional random collisions, but we cannot quantify the amount based on the available information.

Two conclusions can be drawn: (1) the number of collisions is insufficient to thermalize the vibrational degrees of the clusters with the cold helium gas during the expansion, but (2) the number is large enough to cause internal cooling during the expansion. Since the cooling of $T_{\mathrm{vib}}$ is limited [17], a large amount should be attributed to the cooling of $T_{\mathrm{rot}}$. The amount of cooling of $T_{\mathrm{rot}}$ is unknown and source dependent.

### E. Temperature from source to quitting surface

The measured velocity distributions contain for every mass information about both the flow velocity and the translational temperature, which is clear if one rewrites Eq. (7) as

$$f_{q,\mathrm{clus}}(v_{x,\mathrm{clus}}) dv_{x,\mathrm{clus}} \propto \exp\left(-\frac{m_{\mathrm{clus}}(v_{x,\mathrm{clus}} - A)^2}{2k_B B}\right) dv_{x,\mathrm{clus}}, \tag{20}$$

with $A = w_{\mathrm{clus,f}}$ and $B = T_{q,\mathrm{clus}}$, the translational temperature of the clusters in free flight after the quitting surface $q$. $f_{q,\mathrm{clus}}(v_{x,\mathrm{clus}}) dv_{x,\mathrm{clus}}$ with $A = w_{\mathrm{clus,f}}$ differs from the distribution in the source before expansion, where $A = 0$ and $B = T_{S,\mathrm{clus}}(m)$, with $T_{S,\mathrm{clus}}$ being the temperature of the clusters at the moment they leave the source. Depending on the thermalization in the source, $T_{S,\mathrm{clus}}$ may be larger than the temperature of the body of the source, which can be measured by a temperature sensor.

During expansion, chaotic collisions with the rapidly cooling helium can lower the clusters' translational temperature. However, in the fully slipped regime all collisions are systematically accelerating and the distribution cannot change shape, only shift, resulting in $A = w_{\mathrm{clus,f}}$ and $B = T_{S,\mathrm{clus}}$. So, with increasing velocity slip $T_{q,\mathrm{clus}} \to T_{S,\mathrm{clus}}$, and in the fully slipped regime $T_{q,\mathrm{clus}} = T_{S,\mathrm{clus}}$. To determine whether a cluster is in the fully slipped regime, one has to compare its velocity distribution with that of the helium carrier gas. The He flow velocity can be estimated from the fit of Eq. (12) in Fig. 3(b) and is found to be $w_{\mathrm{He}} = (632.5 \pm 1.7)$ m/s. The speed ratio of the monatomic He gas can be estimated to be about $S \approx 25$ by using the approach discussed in Ref. [30] with as input parameters the stagnation pressure, nozzle diameter, and source temperature. The higher the mass of the particles in the helium carrier gas, the lower their flow velocity and thus the larger the velocity slip (see Sec. IV B). This means that, from a large enough mass onwards, the heavy clusters will find themselves in the fully slipped regime.

The fingerprint of thermalization can be defined as $dT_{S,\mathrm{clus}}/dm = 0$. Large particles are fully slipped, so this means that thermalization corresponds to $dT_{q,\mathrm{clus}}/dm \to 0$ for large $m$, with $T_{q,\mathrm{clus}}$ converging to a constant. All clusters smaller than the mass where the converging has occurred

must have a lower temperature because they are cooled by the expanding helium. Full translational thermalization inside the source can only happen if all clusters experience elastic collisions during their time inside of the source, which can only happen if the internal temperature is already equal to the translational temperature of the gas it was colliding with inside the source. Therefore, the only source capable of giving the described fingerprint is a thermalized source.

The widths of the velocity distribution, $v_w$, are plotted in Fig. 3. It is clear that, for large clusters, $v_w$ is not affected by the expansion and still corresponds to the source temperature. It follows a $v_w \propto 1/\sqrt{m}$ model corresponding to a constant temperature in Eq. (6), as proven by the fit in the figure. Figure 4 confirms that the larger clusters indeed find themselves in the fully slipped regime, and still have the temperature of the source. Smaller clusters deviate from this behavior and have a narrower velocity distribution as the one predicted based on the source temperature, which demonstrates that they indeed cool in the expansion.

Complementary information is obtained from the mass dependence of the flow velocity, in Fig. 3(b), large clusters do not achieve the flow velocity needed to have a distribution overlapping with the helium, therefore their collisions are not chaotic and no translational cooling by the helium takes place. However, the flow velocity is much bigger than the elastic case, indicating that the internal degrees of freedom, $T_{\text{vib}}$ and $T_{\text{rot}}$ are being cooled by interactions with the helium. The proportionality constant from the $1/\sqrt{m}$ model is directly related to the source temperature and gives $T_{S,\text{clus}} = (85.9 \pm 1.1)$ K. This value must be compared with the temperature sensors, which read a gradient going from $T_{S,\text{Ext}} = 71$ K to $T_{S,\text{Block}} = 79$ K. This difference of a few kelvin is plausible, the temperature sensor is placed outside of the source, while the inside is heated due to convection of the helium gas and the heat produced by the vaporization lasers. To prove that the conclusions are also valid at other temperatures, the experiment was repeated at a higher source temperature. The results are presented in Appendix D and indeed show comparable behavior for $T_{S,\text{clus}} = (216 \pm 4)$ K. Based on these examples, it is concluded that the source is producing a thermalized cluster distribution. Source thermalization is by no means a given, an example of a nonthermalized source as well as the velocity distributions at different time to free flights in a nonthermalized source can be found in Ref. [38].

## V. CONCLUSION

We have presented a technique to measure the size-dependent velocity distributions of clusters carried by helium gas in a molecular beam. The measured velocity distributions of $Co_n$ ($n < 20$) clusters demonstrate that the translational temperature of larger clusters $Co_n$ ($n \geqslant 20$) remains at the temperature of the source, while smaller clusters undergo a significant translational cooling in the beam. This could be attributed to random collisions of the smaller clusters with the cold helium gas due to their partially overlapping velocity distributions. The cluster's flow velocity is also size dependent, while the flow velocity of the smaller clusters approaches that of the helium gas, the larger clusters have a larger velocity slip. However, the velocity slip is smaller than would be expected for elastic collisions, which implies that the cluster-helium collisions are superelastic.

Average restitution coefficients $C_R$ of cluster-helium collisions are obtained by fitting an elastic model to the flow velocity of the smallest clusters and comparing the actual flow velocity to that predicted by the elastic model. All larger clusters have $C_R$ values above one, which, in combination with theoretical models [5] and the starting temperature upon leaving the source, provides information about the cooling of the cluster's internal temperatures. A significant amount of internal energy is taken away from the clusters, resulting in an increased flow velocity, i.e., the clusters self-accelerate via collisions with the helium. The clusters' vibrational and rotational degrees of freedom cool during the expansion because of a significant number of collisions with the helium gas but do not achieve full thermalization. We did not quantify the internal temperatures of the clusters, because the number of collisions is not precisely known.

The analysis of the size-dependent velocity distributions allows us to determine whether clusters are thermalized when they leave the source. Indeed, if all large clusters have the same translational temperature as the temperature of the source, and the smaller clusters experiencing translational cooling during the expansion have a consistently lower temperature, it can be assumed that all clusters had the same temperature upon leaving the source. The proposed method can be used in different gas-phase setups, where researchers want to know if the produced clusters or molecules are thermalized with the source.

## ACKNOWLEDGMENTS

This work was supported by the Onderzoeksraad, KU Leuven (Project No. C14/18/073). The authors would like to thank Kobe De Knijf, Piero Ferrari, Pepijn Demol, and Kristof Dekimpe for many stimulating discussions.

## APPENDIX A: DERIVATION OF EQ. (9)

If a cluster with velocity $v_2$ is hit by a helium atom with velocity $v_1$, the change in velocity is given by (see Ref. [40])

$$\Delta v_2 = v_2' - v_2 = \frac{C_R m_1 (v_1 - v_2) + m_1 v_1 + m_2 v_2}{m_1 + m_2} - v_2. \tag{A1}$$

This can be rewritten as

$$\Delta v_2 = \frac{m_1}{m_1 + m_2}(C_R + 1)(v_1 - v_2). \tag{A2}$$

If one assumes that the effect of a single collision is small, this corresponds to

$$\frac{dv_2}{dN} = \frac{m_1}{m_1 + m_2}(C_R + 1)(v_1 - v_2), \tag{A3}$$

which can be rewritten as

$$\int \frac{dv_2}{v_1 - v_2} = \frac{m_1}{m_1 + m_2}(C_R + 1) \int dN, \tag{A4}$$

$$-\ln(v_1 - v_2) = \frac{m_1}{m_1 + m_2}(C_R + 1)N + k. \tag{A5}$$

By defining $v_{2,0} = v_2(0)$ as the cluster velocity before any collision and approximating the distribution of helium to be narrow enough to assume $v_1 \approx w_{\mathrm{He}}$, this leads to

$$v_2(N) = w_{\mathrm{He}} + (v_{2,0} - w_{\mathrm{He}}) \exp\left(-N \frac{m_{\mathrm{He}}}{m_{\mathrm{He}} + m_{\mathrm{clus}}}(C_R + 1)\right). \tag{A6}$$

The assumption of a narrow helium velocity distribution, $v_1 \approx w_{\mathrm{He}}$, means that $N$ only takes into account the net number of accelerating collisions.

The flow velocity corresponds to the center of the distribution. Assuming the center of the distribution before acceleration to be at zero velocity, one can find the center of the distribution after acceleration by replacing $v_{2,0}$ in (A6) by zero, and $v_2(N)$ by $w_{\mathrm{clus}}(N)$, finding

$$w_{\mathrm{clus}}(N) = w_{\mathrm{He}}\left[1 - \exp\left(-N \frac{m_{\mathrm{He}}}{m_{\mathrm{He}} + m_{\mathrm{clus}}}(C_R + 1)\right)\right]. \tag{A7}$$

## APPENDIX B: DERIVATION OF EQ. (15)

Equation (14) relates the cluster flow velocity in the elastic case with the real cluster flow velocity and the coefficient of restitution $C_R$:

$$C_R = 2\frac{\ln\left(1 - \frac{w_{\mathrm{clus,f}}}{w_{\mathrm{He}}}\right)}{\ln\left(1 - \frac{w_{\mathrm{clus,el,f}}}{w_{\mathrm{He}}}\right)} - 1. \tag{B1}$$

By definition, the coefficient of restitution is also related to the kinetic energy before and after a collision. The $N$th collision will release an energy given by [see Eq. (11)]

$$\Delta E = \frac{\overline{m}}{2}[w_{\mathrm{clus}}(N) - w_{\mathrm{He}}]^2\left(C_R{}^2 - 1\right). \tag{B2}$$

Thus, the total energy released after $N_{q,\mathrm{net}}$ collisions is

$$E_{\mathrm{released}} = \sum_0^{N_{q,\mathrm{net}}} \Delta E_k = \frac{\overline{m}\left(C_R{}^2 - 1\right)}{2}\left(N_{q,\mathrm{net}} w_{\mathrm{He}}{}^2 - 2w_{\mathrm{He}} \sum_0^{N_{q,\mathrm{net}}} w_{\mathrm{clus}}(N) + \sum_0^{N_{q,\mathrm{net}}} w_{\mathrm{clus}}(N)^2\right). \tag{B3}$$

Using the approximations

$$\sum_0^{N_{q,\mathrm{net}}} w_{\mathrm{clus}}(N) \approx \int_0^{N_{q,\mathrm{net}}} w_{\mathrm{clus}}(N) dN, \tag{B4}$$

$$\sum_0^{N_{q,\mathrm{net}}} w_{\mathrm{clus}}(N)^2 \approx \int_0^{N_{q,\mathrm{net}}} w_{\mathrm{clus}}(N)^2 dN, \tag{B5}$$

one obtains by using Eq. (A7)

$$-2w_{\mathrm{He}} \int_0^{N_{q,\mathrm{net}}} w_{\mathrm{clus}}(N) dN = -2w_{\mathrm{He}}{}^2 \int_0^{N_{q,\mathrm{net}}} \left(1 - e^{-N\frac{m_{\mathrm{He}}}{m_{\mathrm{He}}+m_{\mathrm{clus}}}(C_R+1)}\right) dN = -2N_{q,\mathrm{net}} w_{\mathrm{He}}{}^2 + 2\frac{w_{\mathrm{He}} w_{\mathrm{clus,f}}}{\frac{m_{\mathrm{He}}}{m_{\mathrm{He}}+m_{\mathrm{clus}}}(C_R+1)}, \tag{B6}$$

and

$$\int_0^{N_{q,\mathrm{net}}} w_{\mathrm{clus}}(N)^2 dN = N_{q,\mathrm{net}} w_{\mathrm{He}}{}^2 + \frac{w_{\mathrm{He}}{}^2}{2\frac{m_{\mathrm{He}}}{m_{\mathrm{He}}+m_{\mathrm{clus}}}(C_R+1)}\left[1 - \left(\frac{w_{\mathrm{clus,f}}}{w_{\mathrm{He}}} + 1\right)^2\right]. \tag{B7}$$

Here $w_{\mathrm{clus,f}} \equiv w_{\mathrm{clus}}(N_{q,\mathrm{net}})$. Combining Eqs. (B3), (B6), and (B7) it is found that

$$E_{\mathrm{released}} = m_{\mathrm{clus}}(C_R - 1)\left\{w_{\mathrm{clus,f}} w_{\mathrm{He}} + \frac{w_{\mathrm{He}}{}^2}{4}\left[1 - \left(\frac{w_{\mathrm{clus,f}}}{w_{\mathrm{He}}} + 1\right)^2\right]\right\}. \tag{B8}$$

## APPENDIX C: DERIVATION OF EQ. (18)

To find the collision rate of a pure gas, a common method is to describe the single gas as two gasses moving through each other, with the masses of particles in both gases being identical [30]. First, a few typical velocities need to be defined:

$$v_w = \sqrt{\frac{2k_B T}{m}}, \tag{C1}$$

$$\bar{v} = \sqrt{\frac{8k_B T}{\pi m}} = \frac{2}{\sqrt{\pi}} v_w, \tag{C2}$$

where $v_w$ is the one-dimensional width of the velocity distribution of a gas, as well as the most probable speed when taking the length in three dimensions. $\bar{v}$ is the average speed over all dimensions.

The collision mean-free path of a particle (e.g., a cluster) that moves in another gas (e.g., helium) is given by [30]

$$\bar{\Lambda}_{\mathrm{clus}} = \frac{1}{n_{\mathrm{He}} \sigma_{\mathrm{clus}} \mathrm{Ga}_0}, \tag{C3}$$

where $n_{\mathrm{He}}$ is the helium gas density, and $\sigma_{\mathrm{clus}}$ is the cluster's collision cross section. Furthermore,

$$\mathrm{Ga}_0(s, y) = \Gamma\left(\alpha + \frac{3}{2}\right)\left(1 + \frac{1}{y^2}\right)^{\alpha},$$

$$\text{with } \alpha = \frac{s-3}{2s-2} \quad \text{and} \quad y = \frac{v_{w,\mathrm{clus}}}{v_{w,\mathrm{He}}}. \tag{C4}$$

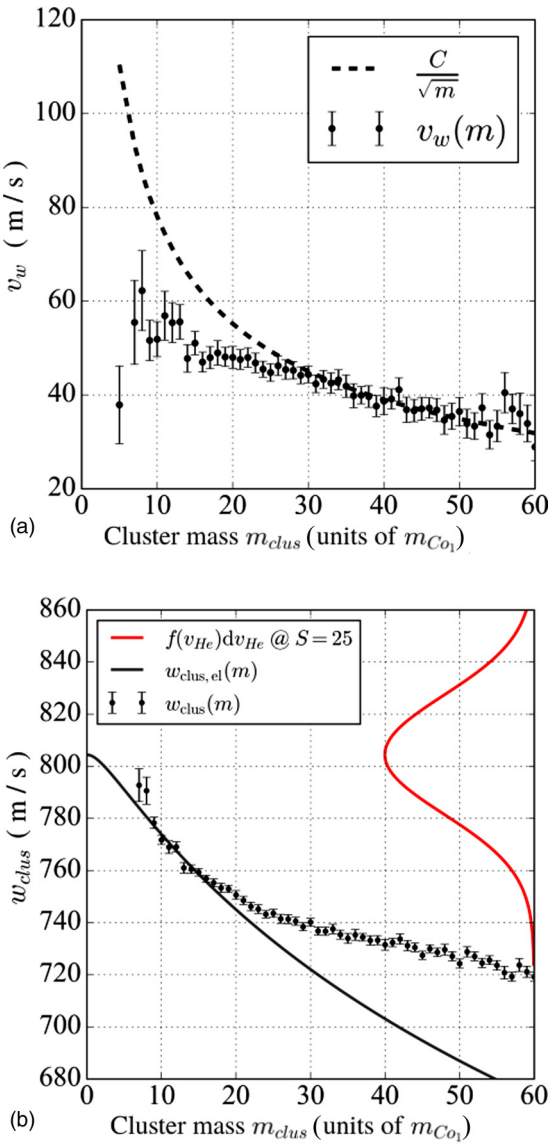


FIG. 8. Velocity distribution measurement of $Co_n$ clusters at a higher source temperature. (a) Width of velocity distribution $v_w$ and (b) cluster flow velocity $w_{clus}$ as a function of the cluster mass. The proportionality constant in panel (a) gives a source temperature of $T_{S,clus} = (216 \pm 4)$ K.

Here $s$ is the exponent for the interaction potential, which for a hard-sphere model $s \to \infty$ is

$$\mathrm{Ga}_0(\infty, y) = \sqrt{1 + \frac{1}{y}}, \tag{C5}$$

since $\alpha \to 1/2$ and $\Gamma(2) = 1$. For a monatomic pure gas, one can simply replace the cluster by a helium atom. In that case $y = 1$ and $\mathrm{Ga}_0(s, y) = \sqrt{2}$. If one has a mixture of two gasses containing atoms of a different mass, like clusters in helium, the equation cannot be simplified.

However, in a mixture of a heavy (clusters) species with an extremely light gas (helium) the equations can be solved. Since $v_w \propto 1/\sqrt{m}$ for clusters, it is possible to make an approximation: $y \ll 1$ and $1/y \gg 1$ (for example if $m_{\mathrm{clus}} = 1000$ u and $m_{\mathrm{He}} = 4$ u, than $y \approx 0.06$), which gives

$$\mathrm{Ga}_0 = \sqrt{\frac{v_{w,\mathrm{He}}}{v_{w,\mathrm{clus}}}}. \tag{C6}$$

One obtains for the two-body collision rate of clusters with helium,

$$Z_{\mathrm{clus}} = \frac{\bar{v}_{\mathrm{clus}}}{\bar{\Lambda}_{\mathrm{clus}}} = \frac{2}{\sqrt{\pi}} \sqrt{v_{w,\mathrm{clus}} v_{w,\mathrm{He}}}\, n_{\mathrm{He}} \sigma_{\mathrm{clus}}, \tag{C7}$$

which can be compared with the collision rate in a pure gas $Z = \sqrt{2}\sigma \bar{v} n$. By using Eqs. (C1), (C7) can be written as

$$Z_{\mathrm{clus}} = \frac{2\sqrt{2k_B}}{\sqrt{\pi}} \sqrt[4]{\frac{T_{\mathrm{clus}} T_{\mathrm{He}}}{m_{\mathrm{clus}} m_{\mathrm{He}}}}\, n_{\mathrm{He}} \sigma_{\mathrm{clus}}. \tag{C8}$$

## APPENDIX D: VELOCITY DISTRIBUTION AT A HIGHER SOURCE TEMPERATURE

The experiment was repeated at a higher source temperature, yielding a temperature of the clusters at the moment they leave the source of $T_{S,\mathrm{clus}} = (216 \pm 4)$ K. The results are presented in Fig. 8 and show a comparable behavior as those in Fig. 3.


[1] P. Ferrari, G. Sanzone, J. Yin, and E. Janssens, in *Nanoalloys: From Fundamentals to Emergent Applications*, edited by F. Calvo (Elsevier, Amsterdam, 2020).

[2] P. Milani and S. Iannotta, *Cluster Beam Synthesis of Nanostructured Materials* (Springer-Verlag, Berlin, Heidelberg, 1999).

[3] W. A. de Heer, Rev. Mod. Phys. **65**, 611 (1993).

[4] M. A. Duncan, Rev. Sci. Instrum. **83**, 041101 (2012).

[5] J. Westergren, H. Grönbeck, A. Rosén, and S. Nordholm, J. Chem. Phys. **109**, 9848 (1998).

[6] Z. Luo, A. W. Castleman, Jr., and S. N. Khanna, Chem. Rev. **116**, 14456 (2016).

[7] E. Janssens, H. T. Le, and P. Lievens, Chem. Eur. J. **21**, 15256 (2015).

[8] M. Andersson, J. L. Persson, and A. Rosén, J. Phys. Chem. **100**, 12222 (1996).

[9] J. De Haeck, N. Veldeman, P. Claes, E. Janssens, M. Andersson, and P. Lievens, J. Phys. Chem. A **115**, 2103 (2011).

[10] S. Heiles, S. Schäfer, and R. Schäfer, J. Chem. Phys. **135**, 034303 (2011).

[11] U. Rohrmann, P. Schwerdtfeger, and R. Schäfer, Phys. Chem. Chem. Phys. **16**, 23952 (2014).

[12] M. Gleditzsch, T. M. Fuchs, and R. Schäfer, J. Phys. Chem. A **123**, 1434 (2019).

[13] A. Diaz-Bachs, M. I. Katsnelson, and A. Kirilyuk, New J. Phys. **20**, 043042 (2018).
[14] V. Zamudio-Bayer, K. Hirsch, A. Langenberg, A. Ławicki, A. Terasaki, B. von Issendorff, and J. T. Lau, J. Phys.: Condens. Matter **30**, 464002 (2018).
[15] I. M. Billas, A. Châtelain, and W. A. de Heer, J. Magn. Magn. Mater. **168**, 64 (1997).
[16] U. Rohrmann and R. Schäfer, Phys. Rev. Lett. **111**, 133401 (2013).
[17] B. A. Collings, A. H. Amrein, D. M. Rayner, and P. A. Hackett, J. Chem. Phys. **99**, 4174 (1993).
[18] G. N. Makarov, Phys. Usp. **54**, 351 (2011).
[19] G. N. Makarov, Phys. Usp. **51**, 319 (2008).
[20] P. Milani and W. A. de Heer, Phys. Rev. B **44**, 8346 (1991).
[21] S. Yang and M. B. Knickelbein, J. Chem. Phys. **93**, 1533 (1990).
[22] D. A. Hales, C. Su, L. Lian, and P. B. Armentrout, J. Chem. Phys. **100**, 1049 (1994).
[23] J. De Haeck, *Mass Spectrometric Developments and a Study of Lithium Doped Silicon and Germanium Clusters*, Ph.D. thesis, KU Leuven, Leuven (2011).
[24] M. B. Knickelbein, J. Chem. Phys. **125**, 044308 (2006).
[25] H. Beijerinck, G. Kaashoek, J. Beijers, and M. Verheijen, Physica B+C (Amsterdam) **121**, 425 (1983).
[26] H. Beijerinck and N. Verster, Physica B+C (Amsterdam) **111**, 327 (1981).
[27] A. Habets, *Supersonic Expansion of Argon into Vacuum*, Ph.D. thesis, Department of Applied Physics, Technische Hogeschool Eindhoven (1977).
[28] R. Campargue, A. Lebehot, and J. Lemonnier, in *Progress in Astronautics and Aeronautics* (AIAA, Reston, VA, 1977), pp. 1033–1045.
[29] G. Brusdeylins, H. Meijer, J. Toennies, and K. Winkelmann, in *Progress in Astronautics and Aeronautics* (AIAA, Reston, VA, 1977), pp. 1047–1059.
[30] H. Pauly, *Atom, Molecule, and Cluster Beams I: Basic Theory, Production and Detection of Thermal Energy Beams*, Springer Series on Atomic, Optical, and Plasma Physics Book 28 (Springer, Berlin, 2012).
[31] E. W. Becker, K. Bier, and H. Burghoff, Z. Naturforsch. A **10**, 565 (1955).
[32] E. W. Becker and W. Henkes, Eur. Phys. J. A **146**, 320 (1956).
[33] M. H. Schwartz and R. P. Andres, in *Progress in Astronautics and Aeronautics* (AIAA, Reston, VA, 1977), pp. 135–147.
[34] T. L. Mazely, G. H. Roehrig, and M. A. Smith, J. Chem. Phys. **103**, 8638 (1995).
[35] S. J. Blundell and K. M. Blundell, *Concepts in Thermal Physics* (Oxford University Press, Oxford, UK, 2006).
[36] G. Niedner-Schatteburg and V. E. Bondybey, Chem. Rev. **100**, 4059 (2000).
[37] P. Ferrari, E. Janssens, P. Lievens, and K. Hansen, Int. Rev. Phys. Chem. **38**, 405 (2019).
[38] J. van der Tol, *Velocities, Temperatures, and Magnetic Moments of Cobalt and Cobalt Dominated Alloy Clusters in Molecular Beams*, Ph.D. thesis, KU Leuven, Leuven (2019).
[39] B. Wrenger and K. H. Meiwes-Broer, Rev. Sci. Instrum. **68**, 2027 (1997).
[40] A. Terry Bahill, *The Science of Baseball: Modeling Bat-Ball Collisions and the Flight of the Ball* (Springer, Berlin, 2018).